Journal of Mathematics and Computing Science, ** (*): **-**, 202*

eISSN: 0128-0767

Stability and Prediction of HFMD Dynamics in Malaysia using an *SIR* Model

Zati Iwani Abdul Manaf[1]* and Nor Atirah Najwa Che Noor Shan [2]

[1,2]Faculty of Computer and Mathematical Sciences, Universiti Teknologi MARA Kelantan Branch, Bukit Ilmu, Machang, Kelantan, Malaysia

Authors' email: zati431@uitm.edu.my*, 2023125977@student.uitm.edu.my

Received **; Received in revised **; Accepted ***
Available online ***
DOI: https://doi.org/10.24191/jmcs.*******

Abstract: Hand, foot, and mouth disease (HFMD) remains a significant public health concern in Asia, with Malaysia and neighbouring countries frequently reporting outbreaks. To better understand its transmission dynamics, this paper applies a Susceptible-Infected-Recovered (SIR) model to HFMD in Malaysia. The analysis focuses on model positivity, equilibrium behaviour, and stability, while the basic reproduction number ( ) is derived using the next-generation method. Two threshold scenarios are considered: when the disease-free equilibrium is stable, indicating eventual eradication, and when the endemic equilibrium is stable, signifying sustained transmission. Numerical simulations support these theoretical results and emphasise the critical role of in shaping outbreak outcomes. A key contribution of this paper is the examination of infection risk variation, showing that higher risks accelerate the shift to endemic persistence, while lower risks extend the stability of the disease-free state. Overall, the findings highlight the importance of threshold dynamics and infection risk in determining HFMD spread. By integrating analytical and numerical approaches, this study offers insights that can inform more effective public health strategies in Malaysia.

Keywords: Basic reproduction number, HFMD, Numerical analysis, *SIR* model, Stability analysis

1 Introduction

Hand-Foot-and-Mouth Disease (HFMD) is a viral infection that continues to pose a serious public health challenge, particularly across Asia [1], [2], [3], [4]. The disease is mainly caused by enteroviruses such as Coxsackievirus A16 (CV-A16) and Enterovirus 71 (EV71). Although HFMD is often mild, major outbreaks have been associated with severe neurological and cardiopulmonary complications [5], [6]. HFMD is also among the most frequently reported notifiable diseases in several countries. For example, China recorded an annual average of 1.87 million cases between 2008 and 2019 [7]. Recurring outbreaks have also been documented in Thailand, Vietnam, Cambodia, and Singapore, underscoring its regional and international significance [6]. Specifically in Malaysia, HFMD has triggered several large-scale outbreaks, including 31 deaths in 1997 and 13 in 2006 [8]. More recent statistics illustrate its persistent threat: Sabah recorded 17,574 cases in 2019 [8], and in 2025, the number of national cases rose by 266% compared to the previous year, with Selangor ranked among the five most affected states [9]. Furthermore, over 80% of cases occur in children under six, particularly in nurseries and preschools where rapid person-to-person transmission is common [8], [9].

Given its recurring nature, mathematical modelling has become an essential tool for analysing HFMD transmission and guiding control strategies [10], [11], [12]. Building on the classical *SIR* model,

numerous studies have examined transmission pathways, estimated reproduction numbers, and evaluated intervention measures. For example, Li et al. [7] analysed age-structured HFMD transmissibility in a major Chinese city and confirmed that children remain the main drivers of spread. In addition, Geng et al. [13] applied multi-input multi-output forecasting in Chengdu, achieving more accurate HFMD predictions than conventional methods. Likewise, Verma et al. [6] extended the *SIR* model into an *SEIRS* framework by incorporating reinfection and seasonal factors to study HFMD in Thailand, while Wongvanich et al. [10] investigated regional residency and optimal control measures in the same setting. More recently, in Malaysia, Adewole et al. [14] recently introduced an age-structured model for children under 15, offering new insights into how age influences epidemic patterns. Overall, these studies highlight the adaptability of mathematical models in capturing the complexity of HFMD transmission and their importance in shaping informed public health responses.

Beyond age- and residency-based approaches, other modelling innovations have also focused on specific biological and ecological aspects of HFMD. For example, Wu [15] examined HFMD dynamics using standard incidence functions, while Chen et al. [5] estimated transmissibility parameters through dynamic modelling. Similarly, Shi et al. [12] studied reaction-diffusion HFMD systems with nonsmooth saturation effects, and Jan et al. [16] investigated fractional-order models with partial immunity. Furthermore, Mohandoss et al. [11] explored the role of vaccination as a control mechanism. Beyond HFMD itself, methods developed for related epidemic models, such as finite-time stability in stochastic *SIR* dynamics [17] and the use of Liénard-Chipart criteria for stability verification [18], provide valuable mathematical tools for extending HFMD modelling analysis. In this regard, such theoretical foundations, as established in classical differential equation frameworks [19], remain central to advancing infectious disease modelling.

Within Malaysia, Nasir and Siam [20] applied the *SIR* model to estimate HFMD transmission parameters from local data. Their work produced useful parameter estimates, and the findings suggested that HFMD may continue to persist in Malaysia. However, stability analysis remains underexplored in their study, which is needed to understand whether the system remains stable over time. In addition, understanding how changes in infection risk might influence the outbreak is also important. Therefore, this research gap motivates the present study. The aims of this study are: (i) to verify the positivity of solutions in the *SIR* framework for HFMD; (ii) to determine the disease-free and endemic equilibrium points; (iii) to derive the basic reproduction number using the next-generation matrix method; and (iv) to validate the analytical findings with numerical simulations under varying infection risk values based on Malaysian 2025 data.

2 Methodology

This section outlines the formulation of the *SIR* model, the theoretical analysis, and the implementation of numerical simulations. The overall research process is illustrated in Figure 1.

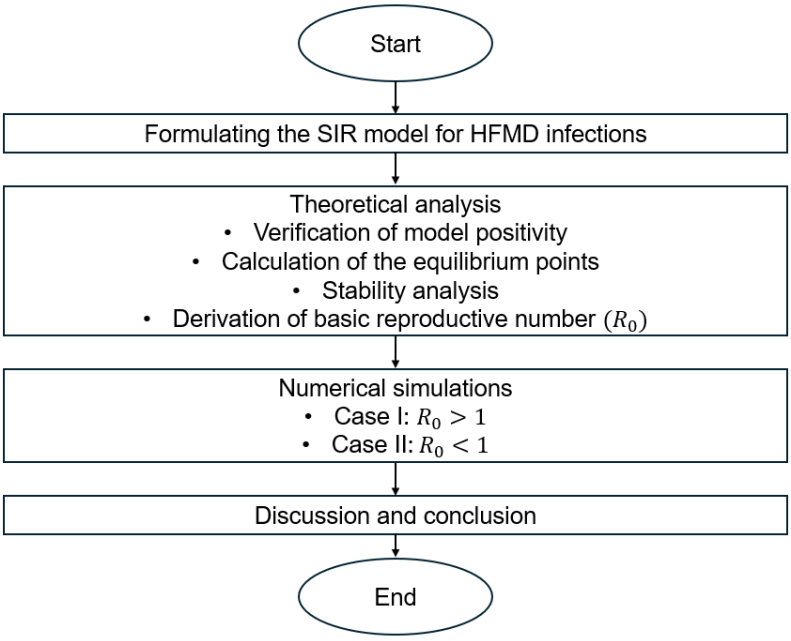

Figure 1: Flowchart of the Research Methodology

A Formulating the SIR Model for HFMD Infections

The formulation of the *SIR* model for HFMD transmission is based on several assumptions. First, the birth rate and natural death rate are assumed to be equal, ensuring that the overall population size remains relatively stable. Second, treatment effectiveness is considered, allowing for the possibility that recovered individuals may lose immunity and return to the susceptible class. Finally, since no deaths have been reported from recent HFMD cases, the disease-related mortality rate is assumed to be very low. Thus, based on these assumptions, the total population is divided into three compartments: susceptible (S), infected (I), and recovered (R), with the total population denoted as (N). The transitions between these compartments are illustrated in Figure 2.

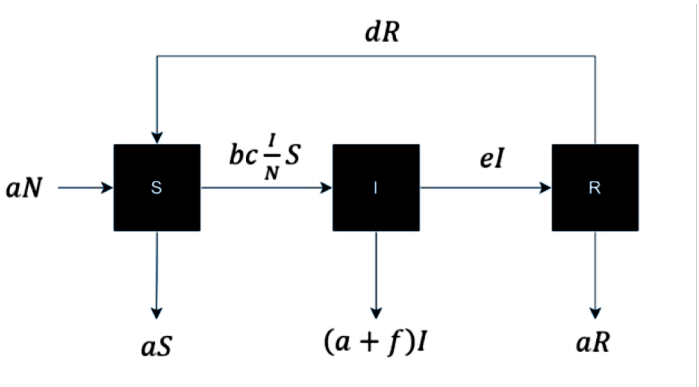

Figure 2: Compartment of SIR model

This classification follows the framework outlined by Nasir and Siam [20]. The interactions among the compartments are represented by the following system of ordinary differential equations (ODEs):

$$\frac{dS}{dt} = aN - \frac{bc}{N}SI - aS + dR \tag{1}$$

$$\frac{dI}{dt} = \frac{bc}{N} SI - (a + e + f) I \tag{2}$$

$$\frac{dR}{dt} = eI - (a + d) R \tag{3}$$

These equations define the rate of change in each compartment, representing the dynamics of HFMD transmission. To ensure biological feasibility, the initial conditions are specified as $S(0) \geq 0$, $I(0) \geq 0$ and $R(0) \geq 0$. These conditions guarantee that the population values remain non-negative throughout the simulation. The parameters used in the system are defined in Table 1.

Table 1: Description of the parameter used in the model

Parameter	Interpretation
a	Rate of population growth and natural death
b	Contact rate between susceptible and infected individuals
c	Risk of infection
d	Proportion of recovered individuals who lose immunity and become susceptible again
e	Recovery rate
f	Death rate from severe illness

The following section presents the theoretical analysis of this system.

B Theoretical Analysis of the SIR Model

This section presents the theoretical analysis of the *SIR* model, focusing on verifying its positivity, determining equilibrium points and their stability, and computing the basic reproduction number using the next-generation matrix method.

i. Positivity of the *SIR* Model

To ensure that the model is biologically meaningful, it is necessary to demonstrate the positivity of the solutions to equations (1), (2), and (3). This condition guarantees that the susceptible, infected, and recovered populations remain non-negative over time, which is essential for epidemiological interpretation.

Theorem 1. *All solutions of the system (1)- (3) with initial conditions* $S(0) \geq 0$, $I(0) \geq 0$ *and* $R(0) \geq 0$ *remain non-negative for all* $t \geq 0$.

Proof. Using the same approach as in [21], the non-negative of the solution can be proved by the equation as follows:

$$S(t) = S(\theta) e^{\int_0^t \left(\frac{aN}{S(\theta)} - \frac{bcI(\theta)}{N} - a + \frac{dR(\theta)}{S} \right) d\theta} \geq 0$$

$$I(t) = I(\theta) e^{\int_0^t \left(\frac{bcI(\theta)}{N} - e - a - f \right) d(\theta)} \geq 0$$

$$R(t) = R(\theta) e^{\int_0^t \left(\frac{eI(\theta)}{R(\theta)} - d - a \right) d(\theta)} \geq 0$$

For any real number and with the initial conditions $S(0) \geq 0$, $I(0) \geq 0$ and $R(0) \geq 0$, it is well known that exponential functions are always non-negative. Consequently, for any time t, each solution of equations (1)-(3) remains non-negative. This completes the proof.

Having established that the model preserves non-negative solutions, the next step is to determine the equilibrium points, which represent the possible long-term states of the system.

ii. Disease-free and Endemic Equilibrium Points

The equilibrium points are calculated by setting the right-hand sides of equations (1)-(3) equal to zero. The disease-free equilibrium (DFE) is obtained by setting $I = 0$, giving:

$$\varepsilon_0 = (N, 0, 0).$$

The endemic equilibrium (EE) occurs where $I \neq 0$, expressed as:

$$\varepsilon_1 = (S^*, I^*, R^*).$$

where:

$$S^* = \frac{N(a+e+f)}{bc},\ I^* = \frac{aN(a+d)(bc-a-e-f)}{bc\left(a^2+a(d+e+f)+df\right)},\ R^* = \frac{aeN(bc-a-e-f)}{bc\left(a^2+a(d+e+f)+df\right)}.$$

These equilibria represent the two possible outcomes of the epidemic: (i) eradication of the infection (DFE) or (ii) persistence of HFMD within the population (EE). Their stability must be analysed to determine which scenario occurs.

iii. Stability Analysis of Disease-free and Endemic Equilibrium

To analyse local stability, the Jacobian matrix of system (1)-(3) is evaluated at each equilibrium point:

$$J(\varepsilon) = \begin{bmatrix} -\frac{bcI}{N} - a & -\frac{bcS}{N} & d \\ \frac{bcI}{N} & \frac{bcS}{N} - e - a - f & 0 \\ 0 & e & -a-d \end{bmatrix}. \tag{5}$$

Subsequently, the equilibrium points can be classified according to their eigenvalues, with further details available in [19]. The following theorems are presented to aid in the analysis of local stability at each equilibrium point.

Theorem 2. *The disease-free equilibrium (DFE) point* $\varepsilon_0 = (N, 0, 0)$ *is locally asymptotically stable if* $bc < a + e + f$.

Proof. The stability of the disease-free equilibrium point is examined by evaluating the eigenvalues of the Jacobian matrix at ε_0. Substituting $\varepsilon_0 = (N, 0, 0)$ into (5) yields:

$$J(\varepsilon_0) = \begin{bmatrix} -a & -bc & d \\ 0 & bc-a-e-f & 0 \\ 0 & e & -a-d \end{bmatrix}.$$

The characteristic equation $|J-\lambda I|=0$ gives the eigenvalues:

$$\lambda_1=-a,\quad \lambda_2=bc-(a+e+f),\quad \lambda_3=-a-d.$$

It is clear that λ_1 and λ_3 are always negative. Therefore, the stability of the disease-free equilibrium depends on λ_2. By requiring $\lambda_2<0$, the condition $bc<a+e+f$ is obtained. Hence, the disease-free equilibrium is locally asymptotically stable under this condition. Hence the proof.

Thus, the DFE is stable only when the infection rate is sufficiently low. When this condition fails, the disease-free state becomes unstable, and the system may approach an endemic state.

Theorem 3. T*he endemic equilibrium (EE) point* $\varepsilon_1=(S^*,I^*,R^*)$ *exists and is locally asymptotically stable if* $bc>a+e+f$.

Proof. The existence of the endemic equilibrium requires $I^*\neq 0$, which holds if $bc>a+e+f$. Substituting this condition into the equilibrium equations gives the positive values of S^*, I^*, R^* as stated. At ε_1, using $\frac{bc}{N}S^*=a+e+f$ and denoting $k=\frac{bc}{N}I^*>0$, the Jacobian becomes:

$$J(\varepsilon_1)=\begin{bmatrix}-(a+k) & -(a+e+f) & d\\ k & 0 & 0\\ 0 & e & -(a+d)\end{bmatrix}.$$

The corresponding characteristic polynomial is $\lambda^3+A_1\lambda^2+A_2\lambda+A_3=0$ with coefficients:

$$A_1=2a+d+k,$$
$$A_2=a^2+ad+(2a+d+e+f)k,$$
$$A_3=k(a^2+ad+ae+af+df).$$

Since $a,d,e,f>0$ and $k>0$, it follows that $A_1>0$ and $A_3>0$. Moreover, expanding $A_1A_2-A_3$ yields only positive terms, ensuring $A_1A_2>A_3$. By the Routh-Hurwitz criterion [11], [15], [16], [18], all eigenvalues have negative real parts. Therefore, the endemic equilibrium ε_1 exist and is locally asymptotically stable whenever $R_0>1$. Hence the proof.

The results above indicate that stability of the equilibria depends critically on the relationship between the transmission rate and the combined removal rates. To make this threshold explicit, the basic reproduction number is now derived.

iv. Basic Reproductive Number

The basic reproduction number, R_0, is derived using the next generation matrix approach [7], [11]. For the infection class I, the rate of new infections is given by $F(I)=\frac{bc}{N}SI$, while the transition terms are $V(I)=(a+e+f)I$. Evaluating the Jacobians at the disease-free equilibrium $\varepsilon_0=(N,0,0)$, yields

$F = bc$ and $V = a + e + f$. The next generation matrix, therefore, reduces to $K = \frac{F}{V}$, and the basic reproduction number is obtained as:

$$R_0 = \frac{bc}{a + e + f}. \tag{6}$$

Corollary. Let $R_0 = \frac{bc}{a + e + f}$ with $a, e, f > 0$. Then, the following are equivalent:

1. If $R_0 < 1$, the disease-free equilibrium $\varepsilon_0 = (N, 0, 0)$ is locally asymptotically stable.
2. If $R_0 > 1$, the disease-free equilibrium $\varepsilon_0 = (N, 0, 0)$ is unstable, and an endemic equilibrium $\varepsilon_1 = (S^*, I^*, R^*)$ exists and is locally asymptotically stable.

Proof. Since $a, e, f > 0$, dividing by $a + e + f$ preserves inequalities:

$$bc < a + e + f \Leftrightarrow R_0 < 1, \quad bc > a + e + f \Leftrightarrow R_0 > 1, \quad bc = a + e + f \Leftrightarrow R_0 = 1.$$

The stability conclusions then follow directly from Theorem 2 (DFE stable when $R_0 < 1$) and Theorem 3 (DFE unstable and EE stable when $R_0 > 1$. Hence, the proof.

3 Results and Discussion

This section validates the analytical findings and presents numerical simulation results. The initial values are based on the total population of Malaysia as of May 2025, estimated at $N = 34.2 \times 10^6$ [22]. The number of HFMD infections at that time was $I(0) = 99,601$ [9], while the initially recovered population was assumed to be zero. Consequently, the susceptible population is calculated as $S(0) = 34,100,399$. Parameter values used in the simulations are adapted from [20] and are summarised in Table 2. Two parameter sets are considered: Case I $(R_0 < 1)$ and Case II $(R_0 > 1)$, representing scenarios below and above the epidemic threshold.

Table 2: Parameter values used in numerical simulations

Parameter	Case I ($R_0 < 1$)	Case II ($R_0 > 1$)
a	0.00022055 $week^{-1}$	0.00022055 $week^{-1}$
b	7.9526 $week^{-1}$	7.5853 $week^{-1}$
c	0.6249 $week^{-1}$	0.9599 $week^{-1}$
d	0.1256 $week^{-1}$	0.3003 $week^{-1}$
e	4.9762 $week^{-1}$	7.000 $week^{-1}$
f	0 $week^{-1}$	0 $week^{-1}$
R_0	0.9986	1.0401

A Validation of Theoretical Analysis

This section validates the theoretical proofs established in Theorems 2 and 3 and the supporting corollary. Table 3 presents the stability analysis for the disease-free equilibrium (DFE) and endemic equilibrium (EE) under both cases.

Table 3: Stability analysis results

Cases	DFE/EE	Eigenvalues	Stability behaviour
Case I ($R_0 < 1$)	$\varepsilon_0 = (N, 0, 0)$	$\lambda_1 = -0.0002205$ $\lambda_2 = -0.006841$ $\lambda_3 = -0.1258$	Asymptotically stable node
	$\varepsilon_1 = (S^*, I^*, R^*)$	$\lambda_1 = 0.006512$ $\lambda_2 = -0.0002206$ $\lambda_3 = -0.1322$	Unstable node
Case II ($R_0 > 1$)	$\varepsilon_0 = (N, 0, 0)$	$\lambda_1 = 0.2809$ $\lambda_2 = -0.0002206$ $\lambda_3 = -0.3005$	Unstable node
	$\varepsilon_1 = (S^*, I^*, R^*)$	$\lambda_1 = -0.1560 + 0.2451i$ $\lambda_2 = -0.0002205$ $\lambda_3 = -0.1560 - 0.2451i$	Asymptotically stable (spiral)

For Case I, the disease-free equilibrium $\varepsilon_0 = (N, 0, 0)$ yields all negative eigenvalues, confirming that the system is a locally asymptotically stable node. This result supports Theorem 2, which states that the DFE is locally asymptotically stable when $R_0 < 1$. At the endemic equilibrium $\varepsilon_1 = (S^*, I^*, R^*)$, however, one eigenvalue is positive, indicating an unstable node. This agrees with the corollary, which asserts that no stable endemic equilibrium exists when $R_0 < 1$.

For Case II, the DFE $\varepsilon_0 = (N, 0, 0)$ becomes unstable because one eigenvalue is positive. This again validates Theorem 2, which predicts instability of the DFE when $R_0 > 1$. In contrast, the endemic equilibrium $\varepsilon_1 = (S^*, I^*, R^*)$ yields eigenvalues with negative real parts, including a complex conjugate pair. This configuration implies that the system approaches equilibrium in an oscillatory manner, forming an asymptotically stable spiral. This finding is consistent with Theorem 3, which establishes that the EE is locally asymptotically stable when $R_0 > 1$. Overall, the numerical stability analysis fully supports the theoretical predictions of Theorems 2 and 3, together with the Corollary. These results confirm that the basic reproduction number R_0 serves as the threshold parameter that determines the local stability of the equilibria.

B Numerical Simulation

This subsection presents numerical simulations to illustrate the system's dynamics under two threshold scenarios: $R_0 < 1$ and $R_0 > 1$. The simulations also examine the effect of varying the infection risk rate, c, on the susceptible, infected, and recovered populations over time. Parameter values are drawn from Table 2, with initial conditions set as $(S_0, I_0, R_0) = (34100399, 99601, 0)$. These values correspond to the Malaysian population as of May 2025 [22], with the HFMD infection level derived from reported data [9]. Figure 3 displays the temporal dynamics of the susceptible, infected, and recovered populations for both cases, with time, t measured in weeks.

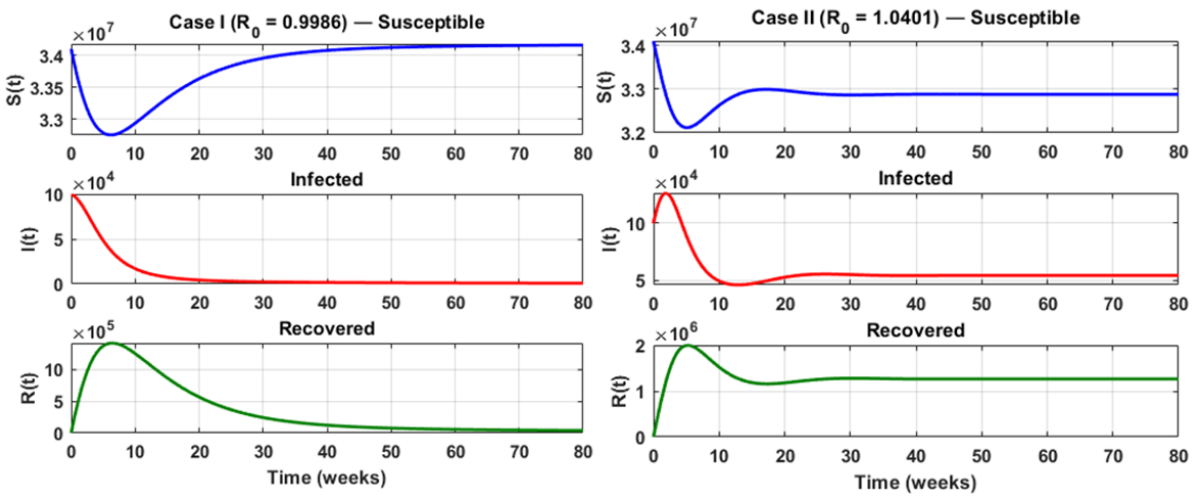

Figure 3: Time series plot for SIR model for Case I ($R_0 = 0.9986 < 1$) and Case II ($R_0 = 1.0401 > 1$)

With initial conditions in May 2025 ($t = 0$), the system begins with approximately 34.1 million susceptibles, 99,600 infected individuals, and no recovered individuals. Two distinct scenarios emerge depending on the value of the basic reproduction number. When $R_0 = 0.9986 < 1$ (Case I), the infection cannot sustain transmission. During the first 10 weeks (May-July 2025), infections decline sharply from nearly 100,000 to fewer than 10,000, and by around week 30 (December 2025), the infected class approaches extinction. In the medium term (July 2025-May 2026, weeks 10-50), the susceptible population increases gradually and stabilises close to 34.2 million, while the recovered class peaks near 100,000 before declining steadily to negligible levels. Over the longer horizon (early-late 2026, weeks 30-80), the system converges to a disease-free equilibrium: infections vanish, the susceptible population persists at ~34.2 million, and the recovered pool stabilises at a very small residual level. Thus, when $R_0 < 1$, HFMD is predicted to die out within seven months (by December 2025), with sustained elimination thereafter.

In contrast, when $R_0 = 1.0401 > 1$ (Case II), the infection persists. During the first five weeks (May-June 2025), the susceptible class declines sharply to about 32.2 million, coinciding with a rapid rise in infections that peak at nearly 120,000 cases around week 4. The recovered population simultaneously increases, reaching 1.8 million by week 8 (July 2025). In the medium term (August 2025-January 2026, weeks 10-30), the system exhibits damped oscillations: the susceptible population gradually rebounds and stabilises near 33 million by week 20, the infected class fluctuates between weeks 15 and 25 before settling at ~50,000 cases, and the recovered class stabilises near 1.5 million by December 2025. Over the longer horizon (early-late 2026, weeks 30-80), the system converges to a stable endemic state, with the susceptible pool remaining above 32 million, the recovered population at ~1.5 million, and infections persisting at a non-zero prevalence of ~50,000. Rather than collapsing, the epidemic transitions into sustained circulation.

Taken together, these scenarios highlight the threshold role of the basic reproduction number in shaping HFMD dynamics in Malaysia. When $R_0 < 1$, the epidemic collapses rapidly, leaving only a negligible number of recovered individuals and restoring the system to a disease-free state. In contrast, when $R_0 > 1$, the infection persists indefinitely, an initial epidemic wave peaks within the first month, followed by damped oscillations and eventual stabilisation at an endemic prevalence of ~50,000 cases from late 2025 onwards. This divergence underscores the critical importance of maintaining effective control measures to $R_0 < 1$, since only under this threshold can HFMD be eradicated rather than entrenched as a recurrent endemic disease.

Next, to further elucidate this threshold behaviour, the infection risk rate, c, is considered, as it plays a crucial role in shaping epidemic trajectories and determining whether a disease will fade out or

persist within the population. Figure 4 presents the time series temporal dynamics of the susceptible $S(t)$, infected $I(t)$, and recovered $R(t)$ populations under three different values of the risk of infection rate parameter c. The red curve corresponds to $c = 0.7519$ ($R_0 = 0.815$), the blue curve to $c = 0.9140$ ($R_0 = 0.990$), and the black curve to $c = 0.9482$ ($R_0 = 1.027$). These curves therefore capture the disease dynamics below the threshold ($R_0 < 1$), at the threshold ($R_0 \approx 1$), and above the threshold ($R_0 > 1$), respectively.

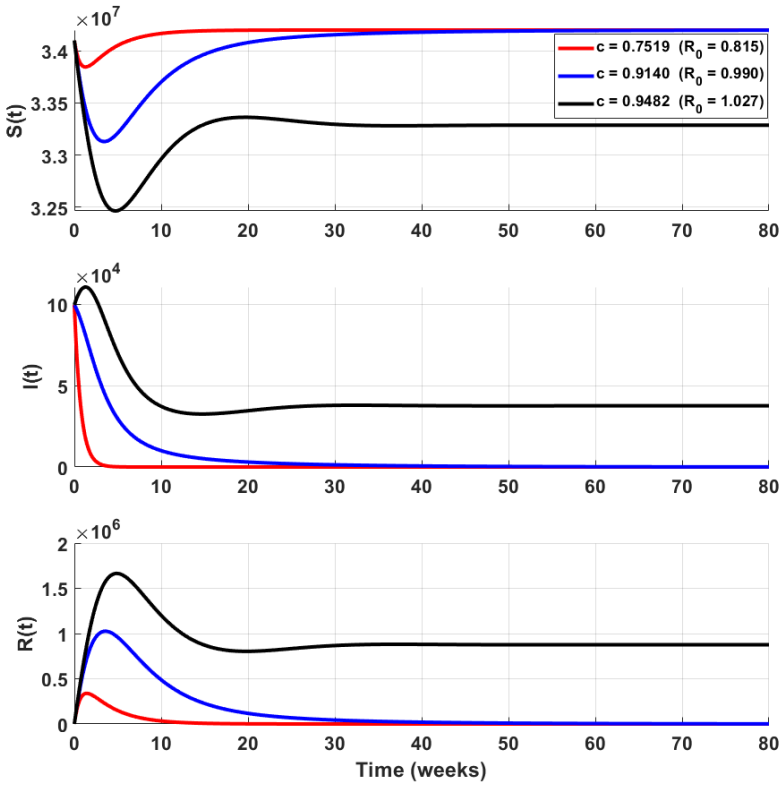

Figure 4: Time series plot when the risk of infection rate, c is varied

When $R_0 = 0.815 < 1$ (red curve), the infection cannot sustain itself. The number of infected individuals $I(t)$ rapidly declines to zero after a small initial peak, and only a small fraction of the population enters the recovered class $R(t)$. Consequently, the susceptible population $S(t)$ returns close to its initial size, reflecting the eradication of the infection. Under this scenario, HFMD in Malaysia is predicted to collapse by July 2025 (week 8), with elimination maintained thereafter.

In the near-threshold scenario ($R_0 = 0.99 \approx 1$, blue curve), the epidemic peak is larger, and the decline of the infected population is slower compared to the sub-threshold case. However, the infection still eventually dies out, leaving a slightly larger recovered population. This outcome suggests that if transmission rates remain marginally below the epidemic threshold, HFMD outbreaks in Malaysia may persist a little longer but will ultimately fade by the end of 2025, without becoming endemic.

Finally, when $R_0 = 1.027 > 1$ (black curve), the infection persists at an endemic level. The infected population $I(t)$ stabilises at a positive equilibrium, the susceptible population $S(t)$ settles below its initial value, and the recovered population $R(t)$ remains significantly elevated. This scenario indicates that if transmission exceeds the threshold, HFMD in Malaysia will not die out but will instead persist as a low-level endemic disease, with recurrent seasonal circulation from late 2025 onwards. Overall, the finding highlights the sharp transition in HFMD outcomes for Malaysia around the epidemic threshold. Small variations in the parameter c close to the critical value can determine whether the infection is eliminated or persists within the population, underscoring the importance of reducing effective contact rates below this threshold through control interventions.

4 Conclusion

This research examined the stability and numerical dynamics of HFMD infections in Malaysia using the *SIR* model. A key contribution lies in demonstrating how small variations in the infection risk rate, c, can shift system behaviour across the epidemic threshold. Three main outcomes emerged: when $R_0 < 1$, the infection dies out within a finite time (around 5-10 weeks in the simulations); when $R_0 \approx 1$, outbreaks persist much longer (20-30 weeks) before fading; and when $R_0 > 1$, the disease becomes endemic, continuing to circulate over the full simulation period. These results highlight how infection risk plays a decisive role in whether an epidemic disappears or becomes established. The findings also showed that values of R_0 just below unity can still produce prolonged outbreaks. For example, at $R_0 = 0.990$, the infection did not vanish immediately but persisted for nearly a year before extinction. This suggests that eradication, while theoretically possible, may demand considerable time and effort, and the disease may appear as though it is continuously present. Such behaviour underscores the need for close monitoring of threshold values and consistent public health strategies to prevent re-emergence.

In addition, this study complements the empirical work of Nasir and Siam [20], who estimated HFMD parameters from Malaysian data and showed that R_0 often remain close to unity. While their work provided direct evidence of HFMD persistence, the present study adds theoretical depth by identifying the stability conditions that explain why such persistence occurs. Moreover, the main novelty of this study is the examination of infection-risk variation, supported by numerical simulations based on Malaysian 2025 outbreak data. Taken together, these studies offer a fuller picture: empirical results demonstrate HFMD's continued circulation in Malaysia, while the current analysis clarifies the underlying dynamics that determine whether the disease moves toward elimination or becomes endemic. The results further show that even modest interventions can significantly alter epidemic patterns and shorten outbreak duration. For example, reducing the infection-risk parameter by small margins can shift outbreak persistence from almost 30 weeks to extinction within 10 weeks. Measures such as promoting hygiene in schools and childcare centres, encouraging early case isolation, and maintaining preventive campaigns can therefore substantially limit HFMD transmission. The sensitivity of HFMD spread to small parameter changes highlights the importance of continuous preventive efforts rather than reactive responses.

Future work could strengthen these insights by incorporating age-specific contact structures. In particular, integrating stability analysis with real-time outbreak data would allow prediction not only of whether HFMD persists but also for how long, thus supporting adaptive interventions. Such efforts would enhance the ability to design timely and evidence-based control strategies for HFMD in Malaysia and comparable settings.

Acknowledgements

The author would like to thank the editor and reviewers for their thorough reading of the original manuscript and their numerous helpful comments and recommendations, which substantially enhanced the presentation of this work.

Conflict of Interest Statement

The authors agree that this research was conducted in the absence of any self-benefits, commercial or financial conflicts and declare the absence of conflicting interests with the funders.

Author Contributions

Zati Iwani Abdul Manaf contributed to the conception and design of the study, performed the data analysis, interpreted the results, and revised the manuscript. Nor Atirah Najwa Che Noor Shan contributed to the data analysis and interpretation and was responsible for drafting the initial version of the manuscript.

References

[1] S. Tikute and M. Lavania, "Hand, foot, and mouth disease (HFMD) in India: A review on clinical manifestations, molecular epidemiology, pathogenesis, and prevention," *Indian Dermatol Online J*, vol. 14, no. 4, p. 475, 2023, doi: 10.4103/idoj.idoj_423_22.

[2] Y. Zhang, "Epidemics of Hand, Foot, and Mouth Disease," in *Molecular Biology of Hand-Foot-Mouth Diseases*, Singapore: Springer Nature Singapore, 2024, pp. 1–27. doi: 10.1007/978-981-99-9660-5_1.

[3] M. Y. Pong, J. F. Yap, and M. Jikal, "Epidemiology of hand, foot and mouth disease outbreaks in Sabah, Malaysia: One year cross-sectional study," *IJID Regions*, vol. 14, p. 100543, Mar. 2025, doi: 10.1016/j.ijregi.2024.100543.

[4] P. Zhu *et al.*, "Current status of hand-foot-and-mouth disease," *J Biomed Sci*, vol. 30, no. 1, p. 15, Feb. 2023, doi: 10.1186/s12929-023-00908-4.

[5] S. Chen, D. Yang, R. Liu, J. Zhao, K. Yang, and T. Chen, "Estimating the transmissibility of hand, foot, and mouth disease by a dynamic model," *Public Health*, vol. 174, pp. 42–48, 2019, doi: https://doi.org/10.1016/j.puhe.2019.05.032.

[6] S. Verma *et al.*, "Hand, Foot, and Mouth Disease in Thailand: A Comprehensive Modelling of Epidemic Dynamics," *Comput Math Methods Med*, vol. 2021, pp. 1–15, Mar. 2021, doi: 10.1155/2021/6697522.

[7] P. Li *et al.*, "Analysis of HFMD Transmissibility Among the Whole Population and Age Groups in a Large City of China," *Front Public Health*, vol. 10, Apr. 2022, doi: 10.3389/fpubh.2022.850369.

[8] S. Y. Fong *et al.*, "A five-year retrospective study on the epidemiology of hand, foot and mouth disease in Sabah, Malaysia," *Sci Rep*, vol. 11, no. 1, p. 17814, Sep. 2021, doi: 10.1038/s41598-021-96083-3.

[9] Z. A. Mutalib, "HFMD melonjak 266 peratus, Selangor antara 5 negeri catat kes tertinggi," *BH ONLINE*, May 12, 2025. [Online]. Available: https://www.bharian.com.my/berita/nasional/2025/05/1395124/hfmd-melonjak-266-peratus-selangor-antara-5-negeri-catat-kes

[10] N. Wongvanich, I.-M. Tang, M.-A. Dubois, and P. Pongsumpun, "Mathematical Modeling and Optimal Control of the Hand Foot Mouth Disease Affected by Regional Residency in Thailand," *Mathematics*, vol. 9, no. 22, 2021, doi: 10.3390/math9222863.

[11] A. Mohandoss, G. Chandrasekar, and R. Jan, "Modelling and Analysis of Vaccination Effects on Hand, Foot, and Mouth Disease Transmission Dynamics," *Mathematical Modelling of Engineering Problems*, vol. 10, no. 6, Dec. 2023, doi: 10.18280/mmep.100603.

[12] L. Shi, H. Zhao, and D. Wu, "Dynamical analysis for a reaction-diffusion HFMD model with nonsmooth saturation treatment function," *Commun Nonlinear Sci Numer Simul*, vol. 95, p. 105593, 2021, doi: https://doi.org/10.1016/j.cnsns.2020.105593.

[13] X. Geng *et al.*, "Evaluation of models for multi-step forecasting of hand, foot and mouth disease using multi-input multi-output: A case study of Chengdu, China," *PLoS Negl Trop Dis*, vol. 17, no. 9, p. e0011587, Sep. 2023, doi: 10.1371/journal.pntd.0011587.

[14] M. O. Adewole, F. A. Abdullah, and M. K. M. Ali, "Dynamics of hand, foot and mouth disease in children under 15 years old: A case study of Malaysia using age-structured modelling approach," *Appl Math Model*, vol. 125, pp. 728–749, 2024, doi: https://doi.org/10.1016/j.apm.2023.10.002.

[15] C. Wu, "Analysis of a Hand-Foot-Mouth Disease Model with Standard Incidence Rate and Estimation for Basic Reproduction Number," *Mathematical and Computational Applications*, vol. 22, no. 2, p. 29, Apr. 2017, doi: 10.3390/mca22020029.

[16] R. Jan, S. Boulaaras, S. Alyobi, and M. Jawad, "Transmission dynamics of Hand–Foot–Mouth Disease with partial immunity through non-integer derivative," *International Journal of Biomathematics*, vol. 16, no. 06, Aug. 2023, doi: 10.1142/S1793524522501157.

[17] N. Gunasekaran, R. Vadivel, G. Zhai, and S. Vinoth, "Finite-time stability analysis and control of stochastic SIR epidemic model: A study of COVID-19," *Biomed Signal Process Control*, vol. 86, p. 105123, 2023, doi: https://doi.org/10.1016/j.bspc.2023.105123.

[18] A. A. M. Daud, "A Note on Lienard-Chipart Criteria and its Application to Epidemic Models," *Mathematics and Statistics*, vol. 9, no. 1, pp. 41–45, Jan. 2021, doi: 10.13189/ms.2021.090107.
[19] W. G. Kelley and A. C. Peterson, *The Theory of Differential Equations*. New York, NY: Springer New York, 2010. doi: 10.1007/978-1-4419-5783-2.
[20] H. Nasir and F. M. Siam, "Parameter estimation of HFMD infection in Malaysia with SIR model," *Annals of Mathematical Modeling*, vol. 3, no. 1, pp. 41–49, Jun. 2023, doi: 10.33292/amm.v3i1.30.
[21] Z. I. Abdul Manaf, S. A. Othman, and W. N. H. Wan Nordin, "The impact of predator attack behaviour on interactions in two-prey and one-predator systems," *Mathematical Sciences and Informatics Journal (MIJ)*, vol. 5, no. 1, pp. 58–71, 2024, doi: 10.24191/mij.v5i1.891.
[22] "The Population of Malaysia," Department of Statistics Malaysia. [Online]. Available: https://open.dosm.gov.my/dashboard/population